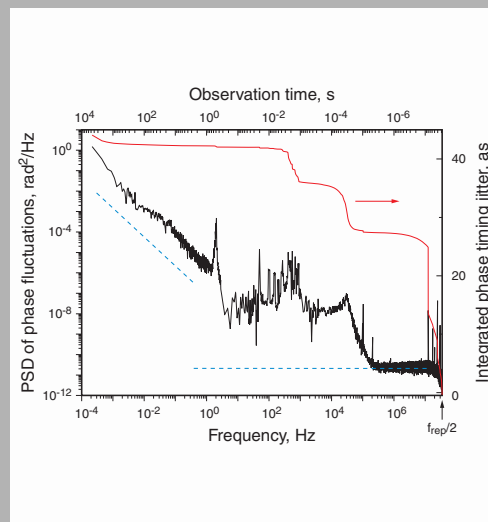


**Abstract:** We demonstrate a novel scheme for carrier-envelope (CE) phase stabilization of few-cycle laser pulses from a mode-locked oscillator. Our scheme utilizes a monolithic, collinear geometry which obviates the need for splitting the laser output, where a fraction is used for CE-phase control and the remainder used for experiment. Rather than using a microstructured fiber and frequency-doubling crystal to generate the beating signal needed for CE-phase locking, in our scheme self-phase modulation and difference-frequency generation occur simultaneously in a single periodically poled lithium niobate (PPLN) crystal and are used to generate equivalent signals. Direct phase-locking and recompression of the output is enabled because the PPLN crystal transmits the majority of the incident fundamental relatively unaffected. As a result, the output provides few-cycle pulses with an unprecedented degree of short- and long-term reproducibility of the electric field waveform. These unique features, along with the simplicity of the scheme make it perfectly suitable for use in seeding CE-phase stabilized amplified laser systems. Results from a 3 kHz amplified Ti:sapphire system will be presented that validate our assertions.



Out-of-loop two-sided phase-noise power spectral density

© 2006 by Astro Ltd.  
Published exclusively by WILEY-VCH Verlag GmbH & Co. KGaA

## Carrier-envelope phase-stabilized amplifier system

J. Rauschenberger,<sup>1,\*</sup> T. Fuji,<sup>1</sup> M. Hentschel,<sup>2</sup> A.-J. Verhoef,<sup>1</sup> T. Udem,<sup>1</sup> C. Gohle,<sup>1</sup> T.W. Hänsch,<sup>1,3</sup> and F. Krausz<sup>1,3</sup>

<sup>1</sup> Max-Planck-Institute of Quantum Optics, Hans-Kopfermann-Strasse 1, D-85748 Garching, Germany

<sup>2</sup> Femtolasers Produktions GmbH, Fernkorngasse 10, A-1100 Vienna, Austria

<sup>3</sup> Ludwig-Maximilians-Universität München, Am Coulombwall 1, D-85748 Garching, Germany

Received: 30 August 2005, Accepted: 3 September 2005

Published online: 16 September 2005

**Key words:** ultrafast processes; optical pulse generation and pulse compression; laser oscillators and amplifiers; higher-order harmonic generation

**PACS:** 42.65.Re, 42.60.Da, 42.65.Ky

Control of the carrier-envelope (CE) phase of amplified ( $\sim$ mJ) few-cycle light pulses is required for reproducible generation of isolated sub-femtosecond XUV/soft-x-ray pulses that can be used to pump or probe electron dynamics deep in the interior of atoms and molecules. In the first proof-of-principle experiments, intense phase-controlled few-cycle laser pulses [1,2] were used to produce isolated 250 attosecond (as) pulses at photon energies near 100 eV [3] by means of high harmonic generation (HHG). In the future, access to a wider range of electronic dynamics within core shells will require even shorter and more energetic x-ray pulses. Intense few-cycle

laser pulses of  $\sim$ 5 fs duration, whose electric field waveform is controlled with respect to the pulse envelope peak with accuracy of 100 as or better, are necessary in order to produce useful probe pulses via HHG. Currently, only chirped-pulse amplifier (CPA) systems that incorporate two CE-phase-stabilization loops have been demonstrated to be useful for this purpose. These lasers employ a phase-stabilized oscillator to seed a CPA power amplifier, which is then phase, corrected with a secondary, feedback phase stabilization loop. Optical parametric chirped-pulse amplification with phase control has been demonstrated [4], however to date the pulse duration of these systems

\* Corresponding author: e-mail: jens.rauschenberger@mpq.mpg.de

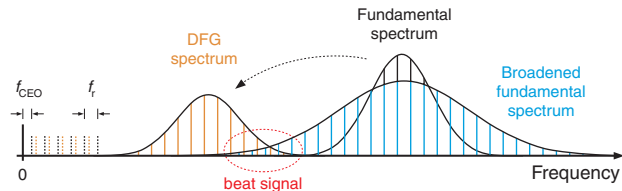


**Figure 1** (online color at [www.lphys.org](http://www.lphys.org)) Principle of  $f_{CEO}$  detection: an additional frequency comb,  $f_m = mf_r$  with  $f_{CEO} \equiv 0$  is created in a nonlinear crystal by DFG. The frequency comb of the seed laser  $f_n = nf_r + f_{CEO}$  is spectrally broadened by SPM. With  $k$ ,  $m$ , and  $n$  being integers, the combs partially overlap to produce heterodyne beat notes at  $f_{beat} = \pm|nf_r + f_{CEO} - mf_r| = kf_r \pm f_{CEO}$

remains around 10 fs. Phase stabilization of an ultrashort laser oscillator is of primary concern. The most widely used technique for stabilization of the CE offset frequency ( $f_{CEO}$ ) of a femtosecond oscillator, the frequency at which the CE phase reproduces itself, is to measure the interference beat signal between the high-frequency and the second harmonic of the low-frequency spectral components of an octave-spanning spectrum and phase-lock it to a reference clock [5–9]. This scheme, termed the  $f$ -to- $2f$  self-referencing method, uses an auxiliary beam split from the main laser oscillator, which is then broadened with a microstructured optical fiber to span a full octave. However effective it is, there are several drawbacks to this technique. Most importantly, phase jitter will accumulate between the actual laser output and that used in the phase-stabilization setup, which will compromise experiments performed with this laser. Moreover, the  $f$ -to- $2f$  self-referencing method is non-collinear; as a result it is highly sensitive to alignment, which introduces additional phase jitter. Furthermore, a substantial portion of the oscillator output is required for broadening in a microstructured fiber.

Here, a different approach to phase-stabilization of a mode-locked oscillator is presented that allows for CE-phase stabilization directly in the usable laser output, resulting in lower CE-phase jitter [10].

By tightly focusing few-cycle pulses from a Ti:sapphire oscillator into a highly nonlinear magnesium-oxide-doped periodically poled lithium niobate (PP-MgO:LN) crystal, self-phase modulation (SPM) and difference-frequency generation (DFG) occur simultaneously (see Fig. 1). In the region of spectral overlap, an interferometric beat signal can be detected. Due to the absence of walk-off effects and improved spatial overlap, the nonlinear interaction between the two waves in the crystal is enhanced, making the beating signal strong enough for reliable CE-phase locking.

The CEO beat signal is easily isolated because it exists outside the original laser spectrum, and the relatively moderate dispersion in the nonlinear crystal allows for the recompression of the transmitted laser pulses. The implica-

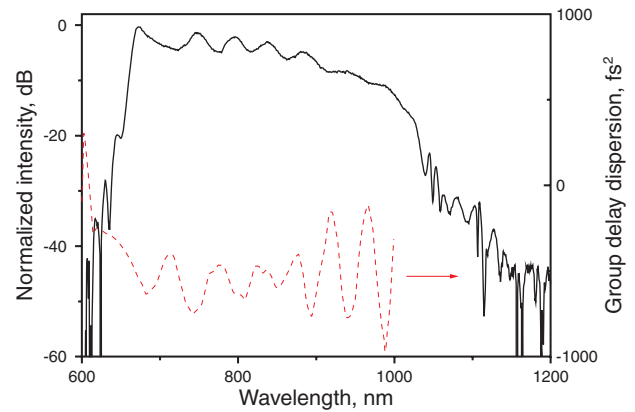


**Figure 2** (online color at [www.lphys.org](http://www.lphys.org)) Spectrum generated by the oscillator (solid curve), measured with a scanning monochromator and net intracavity group-delay dispersion (dotted curve)

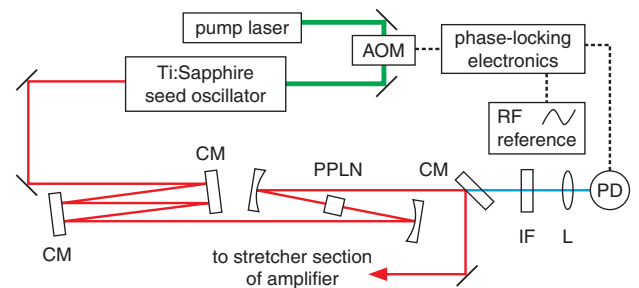


**Figure 3** (online color at [www.lphys.org](http://www.lphys.org)) Experimental realization of the monolithic CE-phase stabilization scheme. CM: chirped mirror; IF: long-pass filter (cutoff 1400 nm); L: lens; PD: InGaAs photodiode; RF reference: signal generator; and AOM: acousto-optic modulator

tions are numerous and far reaching: (i) the full laser power is used for inducing the nonlinear processes in the monolithic device, (ii) almost the entire laser power is available for applications such as probing CE-phase-dependent nonlinear processes, absolute frequency measurements or amplifier seeding, (iii) the absence of a microstructured fiber avoids instabilities (amplitude and CE phase) associated with coupling into its tiny core, and (iv), the CE phase is controlled directly in the beam that is used for applications.

The Ti:sapphire oscillator used for this work is based on the prismless oscillator described in [11]. It generates pulses with a spectrum that extends from 660 to 980 nm at -10 dB below its maximum (Fig. 2). Ultra-broadband chirped mirrors are used for dispersion control both inside and outside the cavity and exhibit tailored dispersion over the range of 620–1000 nm. The net round-trip group delay dispersion of the laser resonator is shown in Fig. 2. The average output power of the oscillator is 340 mW at 5.0 W pump power and 78 MHz repetition rate.

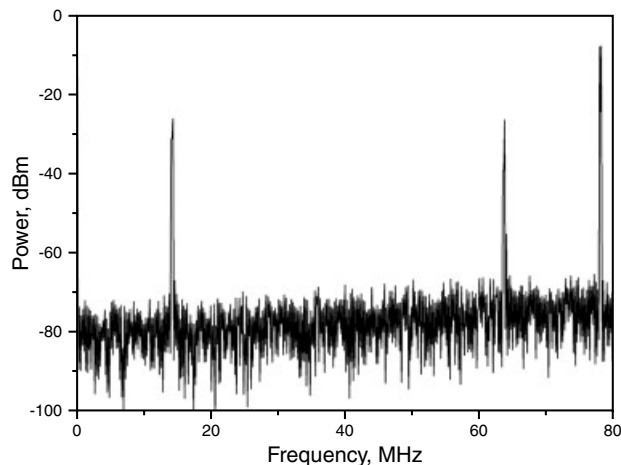


**Figure 4** Pulse train from the nonlinear crystal filtered in the wavelength range of longer than 1400 nm, monitored with a spectrum analyzer. Resolution bandwidth is 100 kHz. Beating signals are visible at 14 and 64 MHz

The experimental setup for the phase-stabilization scheme is shown in Fig. 3. A pair of extra-cavity chirped mirrors compensates for dispersion in the output coupler and compresses the output pulses to  $\sim 6$  fs duration. The pulses are then focused into a 2 mm-long PP-MgO:LN crystal with a poling period of  $11.21 \mu\text{m}$ . A chirped mirror is used as a dichroic beam splitter after the crystal. It reflects the fundamental spectrum and transmits the infrared components of the beam at  $>1250$  nm, which emerge from the nonlinear interactions in the PP-MgO:LN crystal. The transmitted beam is passed through a long-pass filter (1400 nm cutoff) and detected with an InGaAs photodiode.

A characteristic signal from this photodetector is shown in Fig. 4. The beating signal appears in the frequency domain as side-bands on the fundamental of the oscillator repetition rate and its harmonics. The large signal-to-noise ratio (S/N) of more than 50 dB measured with a resolution bandwidth of 100 kHz permits routine locking of the CEO frequency to a reference with the servo loop system described in [9].

The beating between the DFG and SPM waves is observed at  $\lambda > 1350$  nm.

The enhanced spatial and temporal matching of the waves interfering in a monolithic device is expected to improve CE-phase control over that provided by conventional schemes [12–14]. To test the performance, the laser beam that emerges from our setup (Fig. 3) is focused into another PP-MgO:LN crystal for a second independent (out-of-loop) CE-phase measurement. This out-of-loop signal provides an upper limit to the stability of the CE phase, as phase noise added by the locking electronics and both the in-loop and out-of-loop CE-phase detection systems is included. We measured the relative phase of the  $f_{\text{CEO}}$

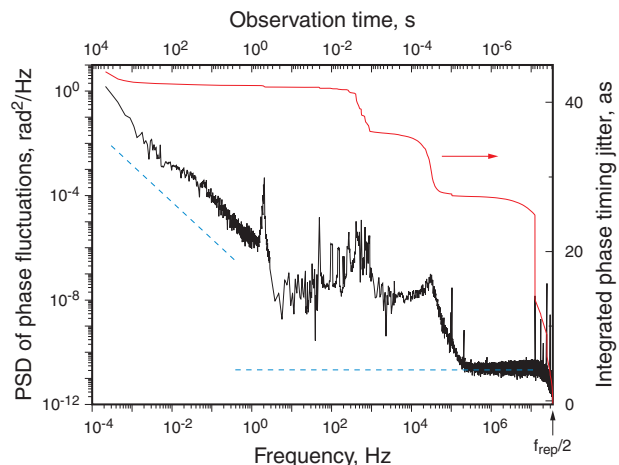


**Figure 5** (online color at [www.lphys.org](http://www.lphys.org)) Out-of-loop two-sided phase-noise power spectral density (PSD),  $S_{\phi}(\nu)$  and integrated CE timing jitter. In a 35 MHz – 0.2 mHz bandwidth, the accumulated timing jitter is 44 as or 99 mrad. The dotted line shows the noise floor of the detection and measurement system

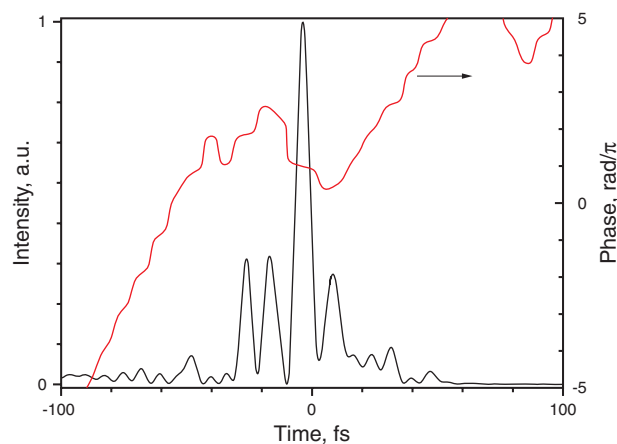


**Figure 6** (online color at [www.lphys.org](http://www.lphys.org)) Temporal profile of the output pulses of the phase-stabilized seed oscillator (passing through the 2 mm length PP-MgO:LN and compressed with chirped mirrors), as retrieved from a SPIDER measurement. The full-width at half maximum of the intensity profile is 5.9 fs

frequency as detected by the two independent  $f_{\text{CEO}}$  detectors. To this end, the first detector was used to lock the  $f_{\text{CEO}}$  beat to an rf reference at 12.5 MHz and the signal of the second  $f_{\text{CEO}}$  detector was used for measuring phase noise. This procedure permits us to measure the temporal variation of the CE-phase,  $\phi(t)$ . The two-sided power spectrum of phase fluctuations,  $S_{\phi}(\nu)d\nu$ , is shown in Fig. 5. The lowest resolved frequency component is given by the inverse of the observation time of 75 min, whereas the highest frequency component is given

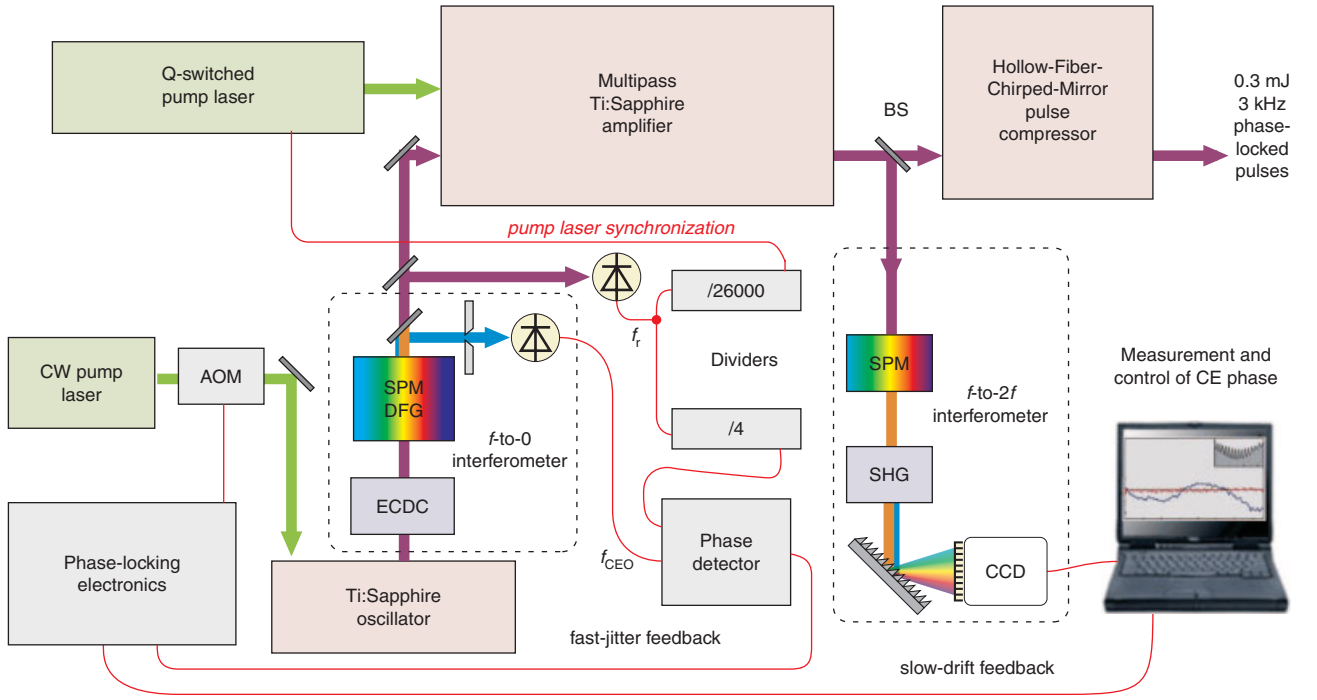


**Figure 7** (online color at [www.lphys.org](http://www.lphys.org)) Schematics of the CE phase-stabilized amplifier setup with the two phase-lock loops shown. AOM: acousto-optic modulator; ECDC: extra-cavity dispersion control; SHG: second harmonic generation; CCD: charge coupled device camera

by  $f_r/2$  ( $f_r$ : repetition rate) according to the Nyquist theorem. The accumulated timing jitter  $\Delta T_{rms}$  as a function of the observation time  $\tau_{obs}$ ,

$$\Delta T_{rms}(\tau_{obs}) = \frac{\lambda_C}{2\pi c} \Delta\phi_{rms}(\tau_{obs}) = \frac{\lambda_C}{2\pi c} \sqrt{2 \int_{1/\tau_{obs}}^{f_r/2} S_\phi(\nu) d\nu}, \quad (1)$$

is also shown in Fig. 5. Here,  $\Delta\phi_{rms}(\tau_{obs})$  denotes the integrated CE phase error and  $\lambda_C$  the center wavelength of the pulses. The phase error integrated from 35 MHz to 0.2 mHz is 99 mrad, or 44 as of timing jitter at the center wavelength of  $\sim 830$  nm. The most comprehensive measurement on a conventional system [14] reports approximately 310 as timing jitter in a 0.9765 mHz – 102.4 kHz frequency band. With the same integration time as used in [14], our integrated phase error would be 77 mrad, corresponding to 34 as of timing jitter and constituting a one order of magnitude improvement.

In the present system, the mirror compressor and the crystal have a combined loss of  $\sim 30\%$ , mainly due to the mirror coating quality and the photorefractive effect in the crystal. The pulse energy after the crystal is approximately 3.3 nJ. Taking into account the large bandwidth of the seed spectrum and the limited gain bandwidth of a Ti:sapphire

amplifier (725–900 nm FWHM), approximately 0.5 nJ is available for seeding a chirped-pulse amplifier.

The dispersion of the PP-MgO:LN crystal can be compensated for by chirped mirrors. The compressed pulses have been characterized with a broadband SPIDER device [15] with the results being summarized in Fig. 6. Serious phase distortions from nonlinear frequency mixing are not present as is verified by comparing the SPIDER results with the crystal being in focus and out of focus. The measurements yielded a pulse width of 5.9 fs, whereas the transform-limited pulse width is 4.8 fs.

The phase-stabilized oscillator serves as a seed in a Ti:sapphire chirped-pulse amplifier system [16–18] (Fig. 7). It consists of a positively-dispersive stretcher, a multipass amplifier and a double prism pair compressor. The multipass amplifier contains a pulse picker (Pockels cell) that reduces the repetition rate to 3 kHz. The high repetition rate of our amplifier in comparison to previously demonstrated amplifier systems greatly simplifies attosecond experiments, because the time needed for data collection is reduced proportionately. The increased repetition rate was reached without cryogenic crystal cooling which can add to the system complexity of the amplifier.

As the CE phase  $\Delta\phi$  is connected to  $f_{CEO}$  by virtue of  $\Delta\phi = 2\pi f_{CEO}/f_r$ , locking  $f_{CEO}$  to a subharmonic of the repetition rate  $f_r$ , say  $f_r/4$ , ensures that every fourth pulse from the seed oscillator has the same CE phase. Subse-

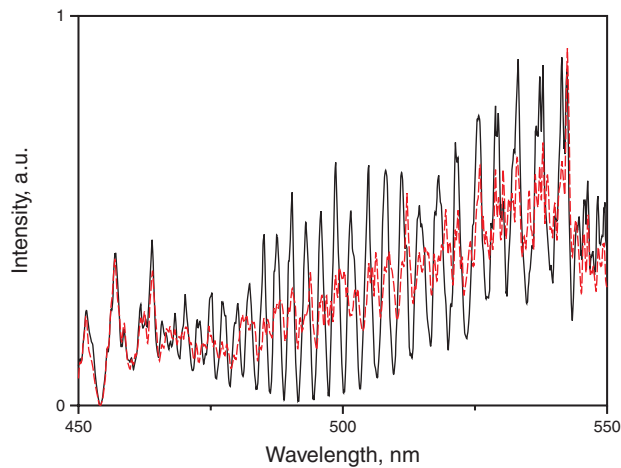


**Figure 8** (online color at www.lphys.org)  $f$ -to- $2f$  interference spectrographs recorded from secondary interferometer, when oscillator phase-locked (solid line) and free running (dashed line). Integration time 20 ms

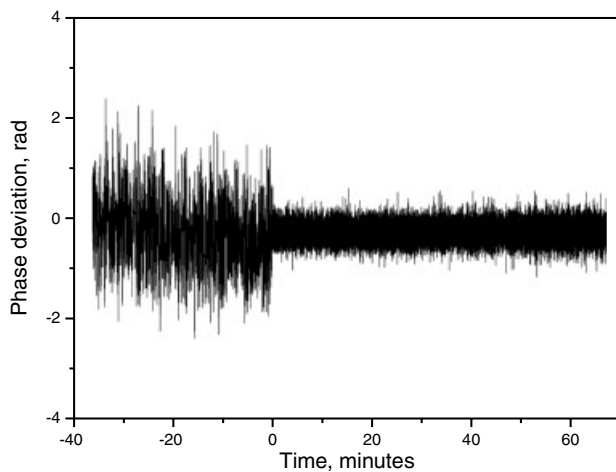


**Figure 9** Phase deviations as derived from the  $f$ -to- $2f$  interference pattern by the Fourier transform algorithm. The secondary feedback loop was put in operation at  $t = 0$ . Root mean square jitter of the locked (unlocked) part of the trace is 149 mrad (678 mrad), in 0.2 mHz – 15 Hz bandwidth

quently by choosing every 26,000th pulse, a 3 kHz pulse train with pulses of identical waveform is generated.

CE phase stability of the amplified pulses is dominated by three factors: Firstly, phase noise from the seed oscillator is transferred directly to the output. Noise components above the picking frequency of 3 kHz are aliased into the picked pulse sequence and can therefore not be neglected [19]. Secondly, pump energy fluctuations contribute by means of intensity-dependent nonlinear phase effects [20]. However, by keeping the B-integral, i.e. the accumulated nonlinear phase in the amplifier, low ( $B \sim 1.1$ ) and by using a low-noise diode-pumped pump laser (amplitude noise

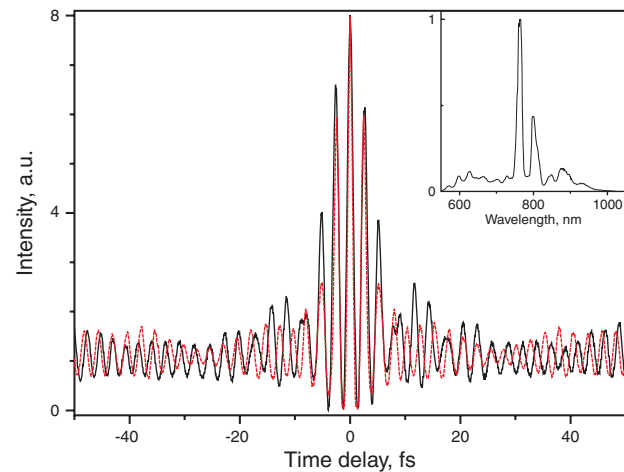


**Figure 10** (online color at www.lphys.org) Autocorrelation trace (solid line) of the pulses after the hollow fiber – mirror compressor. The dashed line shows the transform-limit autocorrelation as derived from the spectrum (inset) assuming flat phase. Full width at half maximum pulse widths are 5.3 fs and 4.4 fs, respectively

<1% rms), this contribution is negligible. Finally, beam pointing instabilities in the amplifier lead to path length fluctuations in the prism compressor, which translate, into CE-phase jitter. Yet, this additional CE phase fluctuation occurs on a slow timescale, i.e. on the order of seconds and can be compensated.

Detection and correction of the additional slow CE phase noise sources is achieved by means of a secondary phase-lock loop, based on  $f$ -to- $2f$  spectral interferometry [2]. For this purpose a small fraction (<1%) of the beam is split off from the main beam after the prism compressor. In this interferometer, an octave-spanning spectrum is easily generated in a sapphire plate. This continuum is then focused into a frequency-doubling crystal and detected with a spectrometer. Appropriate spatial, spectral, and polarization filtering yields an interference pattern in the region of spectral overlap between the short wavelength wing of the fundamental spectrum and the second harmonic signal near  $\lambda \sim 490$  nm.

As expected, the averaged spectrum shows an obvious fringe pattern with high visibility when the seed oscillator is phase-locked (Fig. 8). Slow phase drifts are analyzed by a linear Fourier-transform spectral interferometry algorithm [21]. To correct for these slow phase fluctuations, negative feedback by means of a voltage proportional to the phase deviation is given to the locking electronics of the seed oscillator (see Fig. 7). Fig. 9 shows typical phase deviations recorded in the described manner with both feedback loops in operation. The resulting rms jitter is 149 mrad or 60 as in 0.13 mHz – 15 Hz bandwidth. However, care must be taken, as this does not represent the real fluctuations of the CE phase, as it is recorded within the locking loop. As such, it only shows the effectiveness of the stabilization circuitry [13].

The sub-25 fs, 0.8 mJ pulses from the amplifier are injected into a 1-meter hollow-core fiber filled with noble gas for spectral broadening and compressed by a set of broadband chirped mirrors [22]. By this technique, the system delivers sub-6 fs pulses with 0.3 mJ pulse energy (Fig. 10). Previous experiments [23] showed that the additional CE phase jitter introduced by the hollow-core waveguide is less than 50 mrad rms owing to the small intensity fluctuations of the amplified pulses ( $< 1.5\%$  rms pulse-to-pulse). As a consequence, monitoring the CE phase at the output of the amplifier gives a true indication of the CE phase of the pulses used for attosecond experiments.

In conclusion, we have demonstrated a simple, highly effective monolithic scheme for direct CE-phase stabilization of a mode-locked laser delivering few-cycle pulses. The concept was implemented in a chirped-pulse amplifier system that provides sub-6 fs, 0.3 mJ-pulses at 3 kHz repetition rate. Thus, the light source yields pulses with unprecedented long-term reproducibility of the generated few-cycle waveforms, which may be a key to pushing the frontier of attosecond science to the atomic timescale.

*Acknowledgements* We gratefully acknowledge support from the FWF (Austria) through grants Z63 and P15382, and the European Community's Human Potential Programs under contract MRTN-CT-2003-50138 (XTRA).

## References

- [1] A. Baltuška, T. Udem, M. Uiberacker, et al., *Nature* **421**, 611 (2003).
- [2] A. Baltuška, M. Uiberacker, E. Goulielmakis, et al., *IEEE J. Sel. Top. Quantum Electron.* **9**, 972 (2003).
- [3] R. Kienberger, E. Goulielmakis, M. Uiberacker, et al., *Nature* **427**, 817 (2004).
- [4] R.T. Zinkstok, S. Witte, W. Hogervorst, and K.S.E. Eikema, *Opt. Lett.* **30**, 78 (2005).
- [5] J. Reichert, R. Holzwarth, Th. Udem, and T.W. Hänsch, *Opt. Commun.* **172**, 59 (1999).
- [6] H.R. Telle, G. Steinmeyer, A.E. Dunlop, et al., *Appl. Phys. B* **69**, 327 (1999).
- [7] D.J. Jones, S.A. Diddams, J.K. Ranka, et al., *Science* **288**, 635 (2000).
- [8] R. Holzwarth, Th. Udem, T.W. Hänsch, et al., *Phys. Rev. Lett.* **85**, 2264 (2000).
- [9] A. Poppe, R. Holzwarth, A. Apolonski, et al., *Appl. Phys. B* **72**, 373 (2001).
- [10] T. Fuji, J. Rauschenberger, A. Apolonski, et al., *Opt. Lett.* **30**, 332 (2005).
- [11] T. Fuji, A. Unterhuber, V.S. Yakovlev, et al., *Appl. Phys. B* **77**, 125 (2003).
- [12] F.W. Helbing, G. Steinmeyer, and U. Keller, *IEEE J. Sel. Top. Quantum Electron.* **9**, 1030 (2003).
- [13] S. Witte, R.T. Zinkstok, W. Hogervorst, and K.S.E. Eikema, *Appl. Phys. B* **78**, 5 (2004).
- [14] T.M. Fortier, D.J. Jones, J. Ye, and S.T. Cundiff, *IEEE J. Sel. Top. Quantum Electron.* **9**, 1002 (2003).
- [15] C. Iaconis and I.A. Walmsley, *IEEE J. Quantum Electron.* **35**, 501 (1999).
- [16] D. Strickland and G. Mourou, *Opt. Commun.* **56**, 219 (1985).
- [17] M. Hentschel, Z. Cheng, F. Krausz, and C. Spielmann, *Appl. Phys. B* **70**, S161 (2000).
- [18] S. Sartania, Z. Cheng, M. Lenzner, et al., *Opt. Lett.* **22**, 1562 (1997).
- [19] C. Gohle, J. Rauschenberger, T. Udem, et al., *Opt. Lett.* **30**, 2487 (2005) DOI:10.1364/OL.30.002487.
- [20] C. Corsi and M. Bellini, *Appl. Phys. B* **78**, 31 (2004).
- [21] M. Takeda, H. Ina, and S. Kobayashi, *J. Opt. Soc. Amer.* **72**, 156 (1982).
- [22] M. Nisoli, S. Stagira, S. De Silvestri, et al., *Appl. Phys. B* **65**, 189 (1997).
- [23] A. Ishizawa and H. Nakano, in: T. Kobayashi, T. Okada, T. Kobayashi, K.A. Nelson, and S. De Silvestri (eds.), *Ultrafast Phenomena XIV, Proceedings of the 14th International Conference, Niigata, Japan, July 25-30, 2004* (Springer-Verlag, 2005), p. 37.